# Learning Cross-Sensor Spectral Super-Resolution for Methane Plume Detection over Vegetated Areas Using Sentinel-2 and EMIT Data

**Di Xu[1,2], Philippa J. Mason[2], Jianguo Liu[2], Yanghua Wang[1,2]**

[1]Resource Geophysics Academy, Imperial College London
[1]Department of Earth Science and Engineering, Imperial College London
South Kensington, London SW7 2AZ, UK
d.xu22@imperial.ac.uk

## Abstract

Reliable detection of methane plumes in vegetated regions remains challenging due to the spectral similarity between vegetation reflectance and methane absorption features, as well as the coarse spectral resolution of freely available multispectral satellites such as Sentinel-2. To address this problem, we propose VegiSR, a vegetation-aware spectral super-resolution framework that reconstructs EMIT-like hyperspectral representations from Sentinel-2 imagery. VegiSR leverages cross-sensor spectral learning using a large-scale Sentinel-2 and EMIT paired dataset we constructed, and incorporates a vegetation-aware spectral regularization and spectral attention mechanism to suppress vegetation-induced confusion while enhancing methane-sensitive wavelengths. The reconstructed hyperspectral data is then integrated with matched filter to detect methane plumes in vegetated area where direct Sentinel-2 detection fails. Experimental results demonstrate that VegiSR achieves superior spectral reconstruction fidelity and significantly improves methane detection accuracy over vegetated surfaces compared to U-Net and direct Sentinel-2 methods. This work highlights the potential of cross-sensor spectral super-resolution for global methane monitoring using free multispectral observations.

## Introduction

Methane is an major anthropogenic greenhouse gas, accounting for approximately 20% of global warming (Ocko, Naik, and Paynter 2018). The main sources of anthropogenic methane include oil and gas production, coal mining, landfills, and livestock agriculture (Zavala-Araiza et al. 2017; Karakurt, Aydin, and Aydiner 2012; Bousquet et al. 2006). Although recent identifications of strong methane plumes from large industrial facilities based on satellite remote sensing have substantially improved our understanding of localized high emission events (Duren et al. 2019; Cusworth et al. 2021), methane emissions from vegetated areas, such as agricultural zones near fossil infrastructures, rice paddies, or wetlands, remain poorly characterized. Accurate identification of methane emissions in vegetated regions is crucial to constrain local emission sources and improve regional emission monitoring capabilities (Kyzivat et al. 2022; Karakurt, Aydin, and Aydiner 2012).

Copyright © 2026, Association for the Advancement of Artificial Intelligence (www.aaai.org). All rights reserved.

However, the substantial spectral overlap between vegetation reflectance and methane absorption features in the shortwave infrared bands (SWIRs) makes the detection of methane plumes over vegetated surfaces particularly challenging for traditional multispectral sensors. Recent advances in satellite-based plume detection have predominantly relied on hyperspectral instruments with fine spectral sampling, such as EMIT(Green et al. 2020), AVIRIS-NG(Hamlin et al. 2011), and PRISMA(Vangi et al. 2021). These sensors capture hundreds of narrow spectral bands (typically with 5-10 $nm$ spacing), allowing a fine characterization of methane absorption features near 2.3 $\mu$m. The resulting hyperspectral detail allows an accurate retrieval of methane column concentrations and spatial plume structures. Despite their precision, such instruments suffer from limited spatial and temporal coverage. For instance, EMIT observes only a narrow orbital swath, covering a small fraction of the Earth's surface each month. Consequently, global and continuous methane monitoring remains infeasible when relying solely on hyperspectral observations.

In contrast, multispectral satellite platforms, such as Sentinel-2 (Drusch et al. 2012), with global coverage, high spatial resolution (10–20 m) and a frequent revisit cycle, have shown strong potential for the detection and monitoring of large-scale methane (Ehret et al. 2022; Irakulis-Loitxate et al. 2022; Rouet-Leduc and Hulbert 2024). However, the coarse spectral resolution of Sentinel-2 (13 broad spectral bands) and its lack of contiguous sampling in the SWIRs severely constrain its sensitivity to subtle methane absorption features. Furthermore, vegetation spectral reflectance exhibits strong similarities to methane absorption patterns, particularly around 2100–2400 $nm$, leading to lower discrimination capabilities and frequent false detections. These limitations make direct methane retrieval from Sentinel-2 data unreliable, especially in regions dominated by vegetation.

To overcome these challenges and enable global monitoring of methane emissions from vegetated areas, we propose VegiSR, a cross-sensor spectral learning framework that takes advantage of the complementary strengths of EMIT and Sentinel-2. VegiSR learns a mapping from Sentinel-2's 13 band multispectral observations to the EMIT 285 band hyperspectral domain through a deep spectral super-resolution (SSR) model, based on a modified UNet architec-

ture. Its core innovations are focused on three aspects: (1) a cross-sensor spectral translation mechanism designed to reconstruct fine-grained spectral details, particularly around the 2.3 $\mu$m methane absorption region which are missing in Sentinel-2 imagery; (2) a vegetation-aware spectral regularization module that enhances sensitivity to methane features while suppressing vegetation induction confusion; and (3) the construction of the first large-scale, spatially and temporally co-located Sentinel-2 and EMIT paired dataset, which enables supervised spectral learning between multispectral and hyperspectral domains. After reconstruction, the Matched Filter(MF) algorithm is then applied to generated hyperspectral representations from Sentinel-2 imagery based on VegiSR to achieve reliable methane detection in areas where conventional Sentinel-2 approaches fail. Experimental results on unseen regions demonstrate that the proposed approach effectively generalizes across diverse vegetated landscapes, confirming the feasibility of large-scale methane monitoring using freely available multispectral satellite data.

## Dataset

To enable supervised spectral super-resolution learning between multispectral and hyperspectral observations, we constructed a paired dataset that spatially and temporally aligns Sentinel-2 imagery with EMIT hyperspectral data. To our knowledge, this is the first dataset designed specifically for cross-sensor spectral learning in methane detection in vegetated areas. It integrates hyperspectral observations from the Earth Surface Mineral Dust Source Investigation (EMIT) mission with multispectral Sentinel-2 L1C data provided by the European Space Agency (ESA). EMIT provides surface reflectance across 285 contiguous bands (400–2500 nm) at 60m spatial resolution, while Sentinel-2 offers 13 discrete bands (443–2190 nm) at 10–60 m resolution.

The dataset covers approximately 200 geographically diverse sites from 2023 to 2024 on diverse types of surface, including vegetated, arid, and mixed industrial regions. For each selected scene, EMIT and Sentinel-2 scenes acquired on the same date were paired to ensure temporal consistency. Only image pairs with a spatial overlap of at least 80% were retained. EMIT L1B radiance data were paired with the Sentinel-2 L1C reflectance data to maintain the original spectral integrity before atmospheric correction. Sentinel-2 imagery was resampled to a 60 m spatial grid to match the EMIT ground sampling distance. Spatial co-registration between sensors was performed using geolocation metadata and refined by grid-based alignment on the common coordinate system. Each co-registered pair was subsequently cropped into non-overlapping $200 \times 200$ pixel tiles. Image pairs containing clouds, shadows, or incomplete spatial coverage were manually filtered based on visual inspection, supported by the Sentinel-2 QA60 mask and EMIT quality assurance flags. All reflectance values of the patches were normalized to [0,1] to ensure radiometric consistency between the sensors.

The final dataset contains approximately 8,000 co-registered Sentinel-2 and EMIT image pairs derived from the 200 source locations during 2023-2024. Each sample consists of: (1) a Sentinel-2 multispectral image cube ($H \times W \times 13$), (2) a corresponding EMIT hyperspectral cube ($H \times W \times 285$), (3) a binary vegetation mask derived from the Normalized Difference Vegetation Index (NDVI), used to guide vegetation-aware training, and (4) metadata that include acquisition time, solar zenith angle, and surface type. The pairs are randomly divided into 80% for training, 10% for validation, and 10% for testing. This dataset provides a large-scale benchmark for supervised spectral super-resolution learning for methane detection over vegetated regions.

## Methodology

The proposed framework VegiSR converts Sentinel-2 multispectral data into fine-resolution hyperspectral representations while enabling accurate detection of methane emissions in vegetation dominated regions. As illustrated in Figure 1, the overall framework consists of three major components: (1) a deep spectral super-resolution (SSR) network that learns a spectral transfer from Sentinel-2 to EMIT; (2) a vegetation-aware spectral regularization strategy that enhances separability between methane and vegetation during model training; and (3) a methane detection module that applies a matched filter to the reconstructed hyperspectral spectra for plume localization.

### Spectral Super-Resolution Network

The SSR network is designed to learn a mapping function $f_\theta : X_{S2} \rightarrow Y_{EMIT}$, where $X_{S2} \in R^{H \times W \times 13}$ represents a Sentinel-2 multispectral patch and $Y_{EMIT} \in R^{H \times W \times 285}$ denotes the corresponding EMIT hyperspectral cube. By combining a modified U-Net architecture with spectral attention blocks, the SSR network enables reconstruction of fine spectral details, especially near the 2.3 $\mu$m methane absorption spectral bands.

The proposed model adopts a U-Net architecture (Ronneberger, Fischer, and Brox 2015) as the backbone, consisting of an encoder composed of sequential 2D convolutional blocks and a decoder with transposed convolutional layers for upsampling. The encoder progressively captures multi-scale spatial structures and spectral correlations across Sentinel-2 bands, while the decoder reconstructs the corresponding hyperspectral representations. Skip connections between the encoder and decoder preserve local spatial context and retain low-level spectral information that might otherwise be lost during downsampling.

To further capture inter-band dependencies, a spectral attention module (SAM) is inserted between the encoder and decoder bottlenecks. Inspired by the squeeze and excitation mechanism (Hu, Shen, and Sun 2018), this module performs channel recalibration by learning attention weights $a_c$ for each spectral channel $c$. This process enables the network to adaptively emphasize methane sensitive wavelengths in the shortwave infrared region while suppressing redundant or dominated responses by vegetation, thereby enhancing spectral discrimination capability.

During training, each input patch $X_{S2} \in R^{200 \times 200 \times 13}$ from Sentinel-2 produces a reconstructed hyperspectral cube

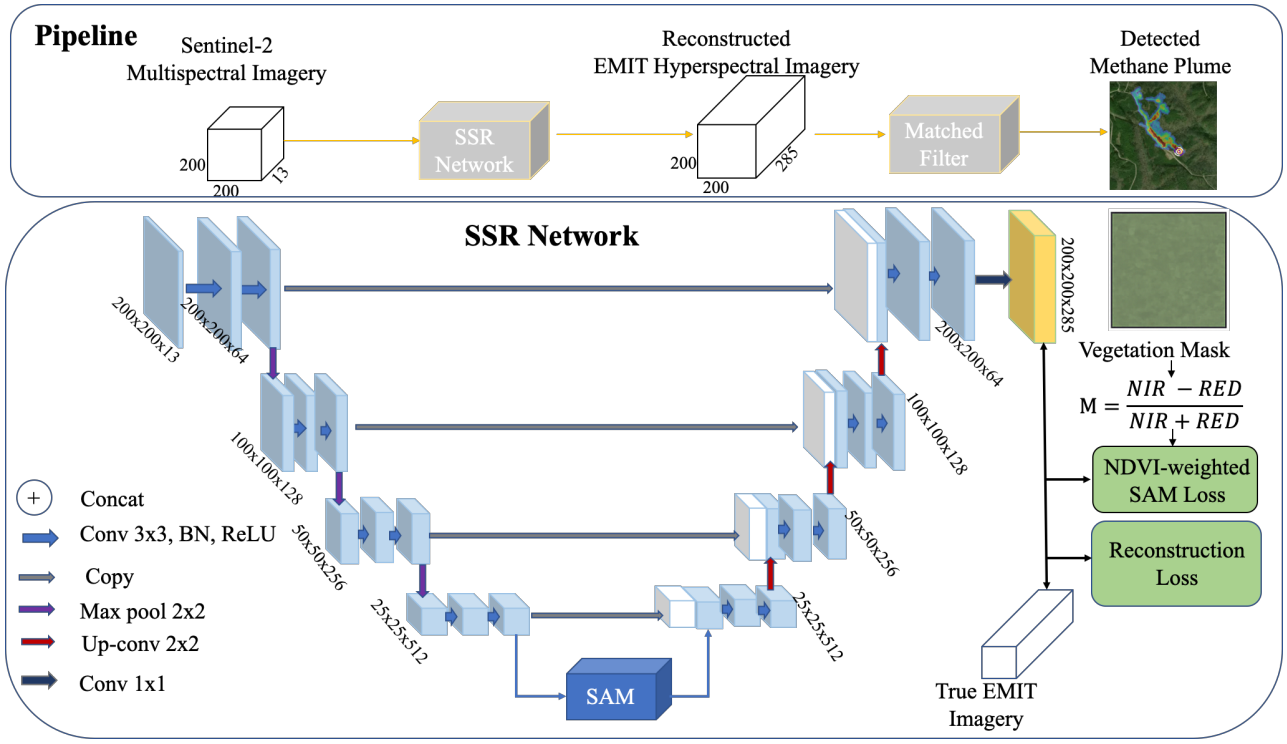


Figure 1: Overview of the proposed VegiSR framework.

$\hat{Y}_{EMIT} \in R^{200\times200\times285}$, which is directly compared against the ground truth EMIT observation $Y_{EMIT}$ using the spectral reconstruction losses described in the next section. The final output layer employs a $1\times1$ convolution to project the decoded feature maps into 285 EMIT bands. Through this supervised spectral learning process, VegiSR effectively transfers EMIT's high spectral fidelity to Sentinel-2 imagery, enabling fine-grained methane-sensitive spectral reconstruction from globally available multispectral data.

## Vegetation-Aware Spectral Regularization

Methane detection in vegetated regions is particularly challenging because vegetation reflectance exhibits absorption patterns similar to those of methane in SWIRs. To reduce vegetation-induced confusion during spectral reconstruction, we incorporate a vegetation-aware regularization strategy at both the loss and feature levels. In addition to the SAM on feature maps, its regularization also combines spatial vegetation masking guided by NDVI (Huang et al. 2021) and spectral loss weighting.

The spatial vegetation mask $M_v$ is derived from the normalized difference vegetation index for each Sentinel-2 patch, computed as:

$$M_v = \frac{NIR - RED}{NIR + RED} \tag{1}$$

where $NIR$ and $RED$ correspond to Sentinel-2 bands centered at 842 nm and 665 nm, respectively. Pixels with $M_v > 0.4$ are classified as vegetation and receive stronger spectral constraints during training.

Furthermore, to encourage the model to preserve angular similarity between the reconstructed and reference spectral, an NDVI-weighted SAM loss is introduced as:

$$\mathcal{L}_{SAM} = \frac{1}{N}\sum_i M_v(i) \cdot \arccos \frac{\langle \hat{Y}_i, Y_i \rangle}{\|\hat{Y}_i\|_2 \|Y_i\|_2} \tag{2}$$

where $\hat{Y}_i$ and $Y_i$ denote the reconstructed and ground truth spectra at pixel $i$. This term penalizes deviations in spectral shape, particularly in areas with rich vegetation. Thus, pixels with high vegetation coverage receive an additional SAM constraint in the loss function. This weighting encourages the model to preserve methane-related absorption characteristics while avoiding overfitting to vegetation reflectance patterns. Therefore, the total training loss combines three components:

$$\mathcal{L}_{total} = \mathcal{L}_{L1} + \lambda_1 \mathcal{L}_{SAM} + \lambda_2 \mathcal{L}_{smooth} \tag{3}$$

where $\mathcal{L}_{L1}$ is the reconstruction loss in pixels, $\mathcal{L}_{SAM}$ is the loss of vegetation weighted spectral, and $\mathcal{L}_{smooth}$ is a regularization of spatial smoothness enforcing local consistency. In all experiments, $\lambda_1 = 0.5$ and $\lambda_2 = 0.1$ were empirically selected.

Together, these mechanisms form a vegetation-aware regularization strategy that improves methane separability in vegetated areas and enhances the robustness of the cross-sensor spectral reconstruction.

## Methane Detection via Matched Filter

After spectral reconstruction, methane plumes are detected using a classical matched filter (MF) approach widely

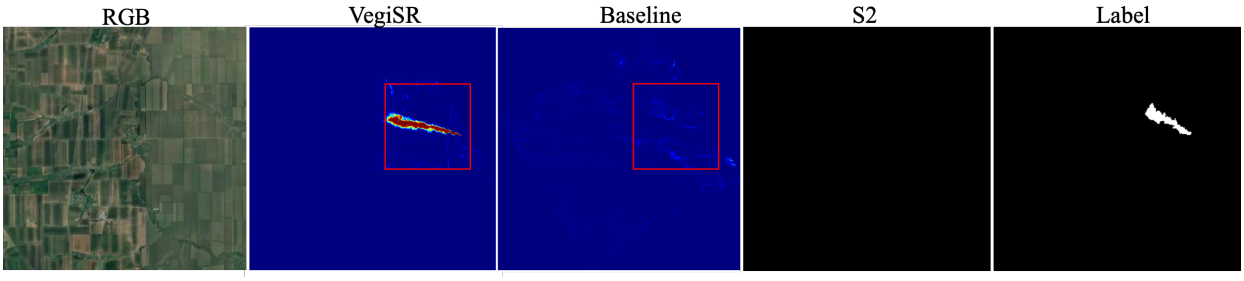


Figure 2: Example detection results in vegetated region. Methane plume detection using matched filtering on reconstructed hyperspectral spectra. RGB: Sentinel-2 true-color composite; VegiSR: SSR reconstruction + MF; Baseline: U-Net reconstruction + MF; S2: Sentinel-2 image + MF; Label: from Carbon Mappper (Duren et al. 2020).

applied in hyperspectral remote sensing(Manolakis et al. 2003). The matched filter estimates the likelihood that a given pixel contains a methane signature by projecting its spectrum onto a reference target signature.

Given a reconstructed hyperspectral spectrum $x$ for each pixel, the matched filter response is computed as:

$$D(x) = \frac{(x - \mu_b)^\top \Sigma_b^{-1} (s - \mu_b)}{(s - \mu_b)^\top \Sigma_b^{-1} (s - \mu_b)} \tag{4}$$

where $x$ is the spectrum of a pixel, $s$ represents the methane absorption spectrum (extracted from EMIT or HITRAN reference data (Gordon et al. 2022)), $\mu_b$ and $\Sigma_b$ denote the mean and covariance of the background spectra, respectively. High filter responses indicate pixels likely to contain methane enhancement.

In summary, the proposed VegiSR framework bridges multispectral and hyperspectral domains by reconstructing EMIT hyperspectral representations from Sentinel-2 imagery, enabling methane plume detection in vegetated regions where hyperspectral coverage is limited. This methodology provides the foundation for global-scale methane monitoring using freely available satellite data.

## Results

We evaluated the performance of VegiSR in both spectral reconstruction and methane detection tasks, and conducted ablation studies to analyze the effectiveness of its key components. In our experiments, VegiSR was implemented in Pytorch and trained on an A100 40GB GPU. The network was trained using AdamW optimizer with an initial learning rate of 5e-4 and weight decay of 0.0025. The batch size was set to 8 and training was performed for 100 epochs with cosine learning rate decay. Loss weights in Eq. 3 were empirically set $\lambda_1$ and $\lambda_2$ at 0.5 and 0.1 respectively. To avoid overfitting, random horizontal and vertical flipping and brightness perturbations were applied as data augmentation.

We first evaluated the spectral reconstruction performance of VegiSR compared to a baseline U-Net architecture without spectral attention or vegetation-aware regularization. Both models were trained on the same Sentinel-2–EMIT paired dataset in identical settings. The reconstructed spectra were quantitatively assessed using the Root Mean Squared Error (RMSE) between the generated and reference EMIT spectra. VegiSR achieved substantially lower RMSE than the baseline U-Net, indicating improved reconstruction accuracy and higher spectral fidelity. The reduction in reconstruction error was most pronounced in the 2100–2400 nm shortwave infrared region, corresponding to the characteristics of methane absorption. This demonstrates that spectral attention and vegetation-based regularization modules effectively enhance the model's ability to recover fine-grained spectral details lost in Sentinel-2 imagery.

To further validate the impact on methane detection, the reconstructed EMIT cube from both VegiSR and the baseline U-Net, and also Sentinel-2 data were used as input to a standard matched filter (MF) algorithm. Figure 2 illustrates qualitative detection results in vegetated regions. While the MF applied to U-Net reconstructions produced several false positives in vegetated areas, VegiSR successfully highlighted methane plumes consistent with EMIT detections, suppressing vegetation-induced artifacts and improving plume localization accuracy. Moreover, due to the coarse spectral resolution of Sentinel-2, directly applying the matched filter on the original multispectral data failed to detect any visible methane plumes, further demonstrating the necessity of the proposed spectral super-resolution framework. These results confirm that VegiSR not only improves spectral reconstruction quality but also translates these improvements into more reliable methane plume detection when combined with conventional hyperspectral analysis methods.

## Conclusion

In this study, we propose a framework, VegiSR, for methane plume detection over vegerated area using free global multispectral imagery. VegiSR leverages cross-sensor spectral learning, a spectral attention module, and a vegetation-aware regularization module to reconstruct EMIT-like hyperspectral representations from Sentinel-2 imagery, enabling accurate methane plume detection over vegetated regions. The model has been validated on the Sentinel-2 and EMIT paired dataset we constructed, showing strong consistency with EMIT observations and superior performance in spectral reconstruction and methane detection. Future work will focus on extending VegiSR to other hyperspectral sensors and improving its adaptability across diverse surface and atmospheric conditions.

## Acknowledgments

The authors are grateful to the sponsors at the Resource Geophysics Academy, Imperial College London, for supporting this research.

## References

Bousquet, P.; Ciais, P.; Miller, J.; Dlugokencky, E. J.; Hauglustaine, D.; Prigent, C.; Van der Werf, G.; Peylin, P.; Brunke, E.-G.; Carouge, C.; et al. 2006. Contribution of anthropogenic and natural sources to atmospheric methane variability. *Nature*, 443(7110): 439–443.

Cusworth, D. H.; Duren, R. M.; Thorpe, A. K.; Olson-Duvall, W.; Heckler, J.; Chapman, J. W.; Eastwood, M. L.; Helmlinger, M. C.; Green, R. O.; Asner, G. P.; et al. 2021. Intermittency of large methane emitters in the Permian Basin. *Environmental Science & Technology Letters*, 8(7): 567–573.

Drusch, M.; Del Bello, U.; Carlier, S.; Colin, O.; Fernandez, V.; Gascon, F.; Hoersch, B.; Isola, C.; Laberinti, P.; Martimort, P.; et al. 2012. Sentinel-2: ESA's optical high-resolution mission for GMES operational services. *Remote sensing of Environment*, 120: 25–36.

Duren, R. M.; Guido, J.; Herner, J.; Rao, S.; Green, R. O.; de Belloy, M.; Schingler, R.; Ardila, D. R.; Thorpe, A. K.; Cusworth, D.; et al. 2020. Carbon Mapper: global tracking of methane and CO 2 point-sources. In *AGU Fall Meeting Abstracts*, volume 2020, A247–01.

Duren, R. M.; Thorpe, A. K.; Foster, K. T.; Rafiq, T.; Hopkins, F. M.; Yadav, V.; Bue, B. D.; Thompson, D. R.; Conley, S.; Colombi, N. K.; et al. 2019. California's methane super-emitters. *Nature*, 575(7781): 180–184.

Ehret, T.; De Truchis, A.; Mazzolini, M.; Morel, J.-M.; D'aspremont, A.; Lauvaux, T.; Duren, R.; Cusworth, D.; and Facciolo, G. 2022. Global tracking and quantification of oil and gas methane emissions from recurrent sentinel-2 imagery. *Environmental science & technology*, 56(14): 10517–10529.

Gordon, I. E.; Rothman, L. S.; Hargreaves, e. R.; Hashemi, R.; Karlovets, E. V.; Skinner, F.; Conway, E. K.; Hill, C.; Kochanov, R. V.; Tan, Y.; et al. 2022. The HITRAN2020 molecular spectroscopic database. *Journal of quantitative spectroscopy and radiative transfer*, 277: 107949.

Green, R. O.; Mahowald, N.; Ung, C.; Thompson, D. R.; Bator, L.; Bennet, M.; Bernas, M.; Blackway, N.; Bradley, C.; Cha, J.; et al. 2020. The Earth surface mineral dust source investigation: An Earth science imaging spectroscopy mission. In *2020 IEEE aerospace conference*, 1–15. IEEE.

Hamlin, L.; Green, R.; Mouroulis, P.; Eastwood, M.; Wilson, D.; Dudik, M.; and Paine, C. 2011. Imaging spectrometer science measurements for terrestrial ecology: AVIRIS and new developments. In *2011 Aerospace conference*, 1–7. IEEE.

Hu, J.; Shen, L.; and Sun, G. 2018. Squeeze-and-excitation networks. In *Proceedings of the IEEE conference on computer vision and pattern recognition*, 7132–7141.

Huang, S.; Tang, L.; Hupy, J. P.; Wang, Y.; and Shao, G. 2021. A commentary review on the use of normalized difference vegetation index (NDVI) in the era of popular remote sensing. *Journal of forestry research*, 32(1): 1–6.

Irakulis-Loitxate, I.; Guanter, L.; Maasakkers, J. D.; Zavala-Araiza, D.; and Aben, I. 2022. Satellites detect abatable super-emissions in one of the world's largest methane hotspot regions. *Environmental science & technology*, 56(4): 2143–2152.

Karakurt, I.; Aydin, G.; and Aydiner, K. 2012. Sources and mitigation of methane emissions by sectors: A critical review. *Renewable energy*, 39(1): 40–48.

Kyzivat, E. D.; Smith, L. C.; Garcia-Tigreros, F.; Huang, C.; Wang, C.; Langhorst, T.; Fayne, J. V.; Harlan, M. E.; Ishitsuka, Y.; Feng, D.; et al. 2022. The importance of lake emergent aquatic vegetation for estimating arctic-boreal methane emissions. *Journal of Geophysical Research: Biogeosciences*, 127(6): e2021JG006635.

Manolakis, D.; Marden, D.; Shaw, G. A.; et al. 2003. Hyperspectral image processing for automatic target detection applications. *Lincoln laboratory journal*, 14(1): 79–116.

Ocko, I. B.; Naik, V.; and Paynter, D. 2018. Rapid and reliable assessment of methane impacts on climate. *Atmospheric Chemistry and Physics*, 18(21): 15555–15568.

Ronneberger, O.; Fischer, P.; and Brox, T. 2015. U-net: Convolutional networks for biomedical image segmentation. In *International Conference on Medical image computing and computer-assisted intervention*, 234–241. Springer.

Rouet-Leduc, B.; and Hulbert, C. 2024. Automatic detection of methane emissions in multispectral satellite imagery using a vision transformer. *Nature Communications*, 15(1): 3801.

Vangi, E.; D'Amico, G.; Francini, S.; Giannetti, F.; Lasserre, B.; Marchetti, M.; and Chirici, G. 2021. The new hyperspectral satellite PRISMA: Imagery for forest types discrimination. *Sensors*, 21(4): 1182.

Zavala-Araiza, D.; Alvarez, R. A.; Lyon, D. R.; Allen, D. T.; Marchese, A. J.; Zimmerle, D. J.; and Hamburg, S. P. 2017. Super-emitters in natural gas infrastructure are caused by abnormal process conditions. *Nature communications*, 8(1): 14012.